Journal of Hydrology (NZ) 35(1): 129-148, 1996

Radiation and ablation on the névé of Franz Josef Glacier

F.M. Kelliher[1], I.F. Owens[2], A.P. Sturman[2], J.N. Byers[1], J.E. Hunt[1], and T.M. McSeveny[1]

[1]*Manaaki Whenua - Landcare Research, P.O. Box 69, Lincoln*

[2]*University of Canterbury, Department of Geography, Christchurch*

Abstract

Radiation and ablation were measured in 0.3 m of recently fallen snow on four consecutive late-summer days under differing weather conditions at 2150-m elevation on the névé of Franz Josef Glacier, New Zealand. Maximum incoming shortwave radiation (R_{si}) was 965 W m^{-2}, with a corresponding outgoing shortwave radiation (R_{so}) of - 675 W m^{-2}. On clear days, albedo (R_{so}/R_{si}) ranged from 0.67 to 0.93 with a daily average of 0.75. The highest values were obtained in the late afternoon. We postulate that hysteresis in the relationship between albedo and solar zenith angle on clear days resulted from early morning hoarfrost that roughened the snow surface, trapping more shortwave radiation than the melting surface film that formed in the afternoon. Under a cloudy sky, albedo was relatively constant at about 0.72. There was generally a net loss of longwave radiation from the snow surface of -50 to -80 W m^{-2}. Net all-wave radiation (R_n) reached a maximum of 160 W m^{-2}, and daily (24 h) total R_n was -0.6 to 0.5 MJ m^{-2} d^{-1}. About 15 % of incident visible radiation penetrated to a depth of 0.07 m in the snow and 1 % to 0.3 m depth. The visible radiation attenuation coefficient was 23 m^{-1}, estimated according to Beer's Law. Over 95% of the 23 mm d^{-1} ablation occurred during daylight, and average daytime R_n = 2.1 MJ m^{-2} was estimated to supply 61% of the energy for surface snow melt.

Introduction

Radiation is a major cause of ablation in temperate alpine glaciers, especially at high elevations (e.g. Hay and Fitzharris, 1988a), and such ablation is fundamentally controlled by the daily radiation cycle (Munro, 1990). Melt-water runoff from glacier basins contributes to total runoff in

many areas of the world. In New Zealand's South Island, seasonal snow storage in alpine catchments that supply hydro-electric storage lakes is usually equivalent to about 15% of annual runoff (Fitzharris, 1987). This is nearly identical to the percentage of runoff generally retained as controlled storage in these lakes. The water is valuable because hydro-generation is used to meet nearly 80% of the national electricity demand (Fitzharris *et al.*, 1992).

In this paper, we examine the primary source of energy transfer processes that affect glacier mass balance and snow melt by studying the micrometeorology of radiation and ablation. Measurements were made in 0.3 m of recently fallen snow on the névé of Franz Josef Glacier, New Zealand, over four consecutive days with variable weather during the late austral summer. We analyse measurements of albedo in conjunction with the fraction of diffuse radiation, solar zenith angle, and snow surface temperature and morphology (e.g. roughness, grain size). Daily radiation balances for the snow surface are constructed from a combination of measured and modelled variables. A simple visible radiation attenuation function for recently fallen snow is developed from light profile measurements. We then explore the connection between radiation and ablation, as measured with an acoustic sensor and also assessed spatially with a network of stakes.

Methods

Study site

The Franz Josef Glacier (latitude 43° 24'S, longitude 170° 12' E) is 10 km long and varies in width from 0.5 km to 7 km. The glacier flows northwest from an accumulation area or névé of about 31 km^2 at an elevation of 1800 - 2700 m, and descends through a steep-sided valley to a terminus at an elevation of about 300 m. Franz Josef Glacier lies on the western slope of New Zealand's Southern Alps, the main axis of which is almost perpendicular to the prevailing westerly winds. The proximity of a vast ocean, combined with orographic effects, leads to abundant precipitation in the névé, estimated to exceed 10 m annually (Griffiths and McSaveney, 1983).

The study site was located at an altitude of 2150 m in the centre of the 200-ha Geikie snow field. The relatively flat snow field is approximately tear-shaped, 3 km long from apex to base in an east-west direction towards the glacier ice fall, and about 1 km wide where we conducted our measurements (Fig. 1). All measurements were made during the late austral summer on 1 - 5 March 1992, beginning one day after a 0.3-m snowfall. There was ice beneath the recently fallen snow, indicating the freezing of

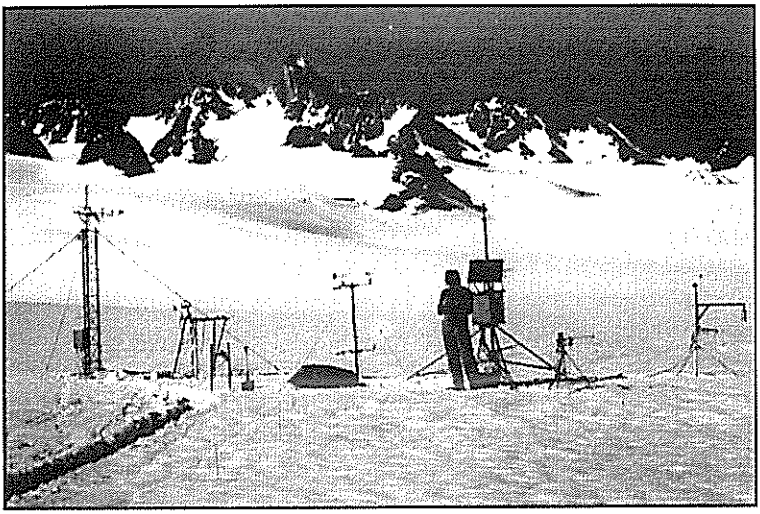

Figure 1 - Instruments for measuring radiation, névé of Franz Josef Glacier (photograph by T.M. McSeveny).

earlier rainfall on the névé surface. The site was at least 300 m above the end-of-summer snowline (Chinn, 1995).

Glacier data tends to be collected during clear and generally calm conditions with little precipitation because of concerns for personal safety and for instrument operation under harsh environmental conditions. Our measurements were conducted over a range of synoptic meteorological conditions typical of those normally experienced in the late summer. A large subtropical anticyclone was located over the Tasman Sea to the northwest of New Zealand, with a gradient southwesterly air flow over the South Island. However, an embedded weak front on 2 March produced a small amount of rain (< 0.2 mm) and significant cloud cover in the afternoon. Consequently, the snow was subject to a change of conditions. By day, total shortwave irradiance reached 965 W m^{-2} and the maximum air temperature was 6 °C. At night, net all-wave radiation was as low as -80 W m^{-2} for up to 12 h, while snow surface temperature reached a minimum of - 10°C.

Measurement and estimation of radiation components

The radiation balance reflects primary energy transfer processes. For a snow surface, it may be expressed:

$$R_n = R_{si} + R_{so} + R_{li} + R_{lo} \qquad (1)$$

where R_n is net all-wave radiation, R_{si} is incoming shortwave radiation,

R_{so} is outgoing (reflected) shortwave radiation, R_{li} is incoming longwave radiation, and R_{lo} is outgoing longwave radiation. All radiation terms are flux densities with units of W m^{-2}. Our surface radiation balance sign convention is positive for incoming and negative for outgoing flux densities. However, for the albedo = R_{so}/R_{si}, we use the conventional positive sign.

A net radiometer (model Q-6, Radiation and Energy Balance Systems, Seattle, Washington USA) was used to measure R_n, and a matched pair of pyranometers (model SP237, BWD Industries, Ltd., Fairfield, Victoria Australia) mounted 0.8 m above the snow for R_{si} and R_{so}. For a view factor of 0.95, the snow surface seen by the downward-facing radiometer sensors had a diameter of 7 m (Reifsnyder, 1967). A third pyranometer placed beneath a shadow band (20-mm wide and 65-mm radius; (Horowitz, 1969)) was used to measure the diffuse component of R_{si}. For cloudless days, the diffuse R_{si} measurements were multiplied by 1.33 to correct for isotropic view-factor and anisotropic sky radiance, calculated after Drummond (1956) and Steven (1984) respectively. For cloudy days, the anisotropic corrections were reduced linearly when cloud cover exceeded 50% according to the results of Stanhill (1985). We estimated cloud cover from the ratio of measured R_{si} to clear-sky R_{si} calculated using a model described by Gates (1980; chapter 6). Our clear-sky radiation model included an atmospheric transmissivity taken from clear sky measurements at the closest available site (0.82 from 600 m elevation at a site 30 km south of Rotorua, New Zealand - latitude 38° 33'S, longitude 176° 25' E). The miminum diffuse R_{si} measurements were multiplied by 1.12 for overcast conditions (Stanhill, 1985).

The reflectance of snow is nearly zero for radiation of wavelengths > 2.5 mm (Male and Granger, 1981), and R_{lo} was determined from the Stefan-Boltzmann Law as:

$$R_{lo} = \varepsilon_s \sigma T_{s0}^4 \qquad (2)$$

where ε_s is the emissivity of snow (0.99, Male and Granger, 1981), σ is the Stefan-Boltzmann constant (5.67 X 10^{-8} W m^{-2} K^{-4}), and T_{s0} is the snow surface temperature (°K). T_{s0} was measured with an infrared radiation thermometer (model AG-42, Telatemp Corporation, Fullerton, California USA) mounted at a height of 0.4 m and pointed towards the south at a 45° angle from the snow surface. Radiation and temperature sensors were connected to data loggers (model 21X, Campbell Scientific, Logan, Utah USA) to obtain 30-min average values.

We made two estimates of R_{li}. The first was a residual calculation from equation (1) using the measurements of R_n, R_{si}, R_{so}, and R_{lo}. The second estimate was based on the Stefan-Boltzmann Law using air temperature (T_a) measured 0.5 m above the snow. For clear skies, an accompanying

effective atmospheric emissivity ε_a was equal to 1.08 [1 - exp{-$\varepsilon_a T_a$/2016}] after Satterlund (1979) where ε_a is vapour pressure, also measured 0.5 m above the snow surface. Half-hourly average T_a and ε_a were measured with a thermocouple and a cooled-mirror dewpoint hygrometer (model DEW-10, General Eastern Instrument Corporation, Watertown, Massachussetts USA). A platinum resistance thermometer embedded in the mirror was used to measure the dew point temperature. Air from an intake 0.5 m above the snow was continuously drawn through separate 2-l mixing chambers at a 0.4 l min^{-1} flow rate. This provided a 5-min averaging time constant. Air from the chambers was alternately switched through the hygrometer every 3 min. The differential thermocouple had 76 mm gauge chromel and constantan wire, was unshielded and naturally ventilated, and a reference junction temperature was measured with a thermistor mounted in the data logger. For overcast conditions during the afternoon of 2 March, atmospheric emissivity was modified after Monteith and Unsworth (1990) to be equal to 1 - [1 - ε_a][4{T_a - T_c}/T_a] where T_c is cloud-base temperature. T_c was approximated to be 2°K cooler than T_a because the cloud base was generally about 200 m above the snow.

We measured the attenuation of visible radiation in recently fallen snow. A slot was dug and photo-diodes (model PH-201A, Nippon Electric Company, Tokyo Japan) were inserted horizontally into small cavities made at depths 0.03, 0.07, 0.11, 0.15, 0.20, and 0.30 m (base of recently fallen snow). The diodes were horizontally scattered over a distance of about 0.3 m to minimise mutual shading. The slot was then re-filled with snow. Immediately after the field measurements, the diodes, pyranometers, and net radiometer were calibrated on the roof of our laboratory for 5 days against a new precision pyranometer (model 8-48, The Eppley Laboratory, Inc., Newport, Rhode Island USA, waveband = 0.285 - 2.8 mm, manufacturer's stated cosine error was ± 2% and 5% for solar zenith angles < 70° and 70 - 80°, respectively).

Measurement of ablation

Ablation or mass loss from the snow pack was determined by measuring the lowering of the snow surface and snow density. This method assumes minimal subsurface melting from radiation penetration (Munro, 1990). Continuous measurements of surface lowering were made with an acoustic sensor (model UDG01, Campbell Scientific, Inc., Logan, Utah USA) placed near the radiation instruments at a height of 1.5 m (far right-hand-side of Fig. 1). An associated environmental variable, wind speed, was measured at a height of 1.8 m using a cup anemometer (model A101m, Vector Instruments, Clwyd United Kingdom). The data were recorded as 30-min averages.

Ablation was also measured at 3-hourly intervals from sunrise until sunset using a steel ruler on 10 white fibreglass stakes placed at 2-m intervals along a pair of undisturbed transects. The stakes were inserted to a depth > 0.3 m into relatively old, dense snow which provided a firm footing. The mean snow surface position was indicated by a 100-mm diameter metal ring placed over the stake and the exposed length of stake was measured with the ruler. Daily observations of snowpack characteristics, including grain form and size and snow density, were made following Colbeck *et al.* (1990).

Results

Shortwave irradiance and albedo

At the study site, only 2% of the sky view factor was occupied by the surrounding, partially snow-covered mountains (calculated from cos2(h), where h is the average horizon elevation angle = 8°; Ishikawa *et al.*, 1992, Fig. 2). The daily path of the sun from 0600 to 1900 h was unobscured, with midday solar zenith angles of 37°. During the measurements, the sky was generally cloudless, except for cloud present during the early morning (0400 - 0630 h) and afternoon (1100 - 1830 h) of 2 March.

On the cloudless days, measured R_{si} was 25 MJ m^{-2} d^{-1} and generally within 10% of that modelled for a clear day (Fig. 3a,c,d and Table 1). There was 6 MJ m^{-2} d^{-1} of diffuse shortwave irradiance. Diurnal variation in the diffuse radiation fraction was significant, with a maximum of about 0.88 to 0.92 near sunrise and sunset, and a minimum of 0.19 from 1000 to 1400 h.

On the partly-cloudy day (2 March) measured R_{si} was 21 MJ m^{-2} d^{-1}, only 76% of the modelled clear sky total (Fig. 3b). The diffuse irradiance was 9 MJ m^{-2} d^{-1} with the diffuse fraction varying from 0.52 to 0.95 during the afternoon, when the cloud base dropped to near the snow surface between 1500 and 1800 h.

The albedo of the recently fallen snow surface was high, ranging from 0.67 to 0.93 (Fig. 4a). There was a small but definite trend of lower minimum albedo as the surface aged from 1 to 4 days (0.70 - 0.67). Surface characteristics, including grain form, grain size, and snow density, changed gradually over the 4-day study (Table 2).

Diurnal variation in albedo was distinctly asymmetrical, particularly on cloud-free days (Fig. 4a). The highest albedos of about 0.90 were obtained during the late afternoon, especially near sunset; early morning maxima were about 0.76, and minimum values occurred about midday. Consequently, there was hysteresis in the relationship between albedo and solar zenith angle (Fig. 5c,d). The lower early-morning albedos were

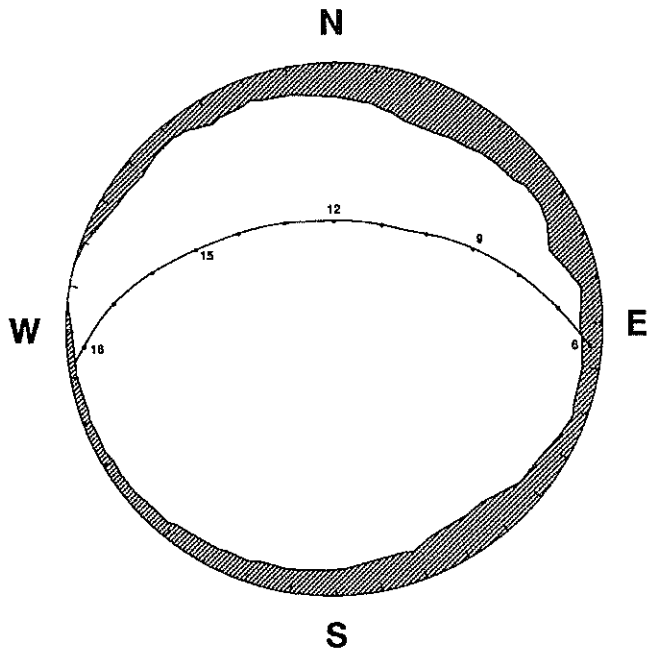

Figure 2 - Polar graph of the horizon and sun path, including hour of the day (solar time), during the study period.

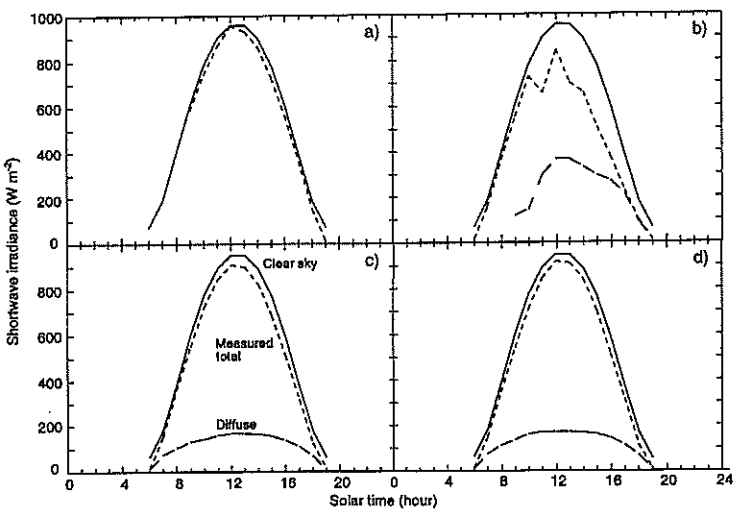

Figure 3 - Hourly averages of modelled clear sky, and measured total and diffuse shortwave irradiance on the névé of Franz Josef Glacier during 1 - 4 March 1992 [a) to d), respectively]

Table 1 - Radiation balances (daytime/daily, MJ m^{-2}) for a recently fallen snow surface on the névé of Franz Josef Glacier. Symbols, calculations, and measurements are described in the text.

March 1992	R_n	Modelled clear-sky R_{si}	Measured total R_{si}	Diffuse R_{si}	R_{so}	R_{lo}	Modelled R_{li}	Calculated Residual R_{li}
1[a]	-/0.5	25.7	23.4	-	-17.1	-/-	-/12.2	-/-
2	1.8/-0.6	27.9	21.2	9.0	-15.5	-14.9/-26.3	11-9/20.9	11.0/20.0
3	2.0/-0.3	27.6	24.9	5.8	-18.1	-15.1/-25.6	12.3/21.1	10.3/18.5
4	2.6/0.5	27.4	24.9	6.0	-17.8	-15.3/-26.1	13.1/22.3	10.2/19.5

[a] 1030 - 2400 h

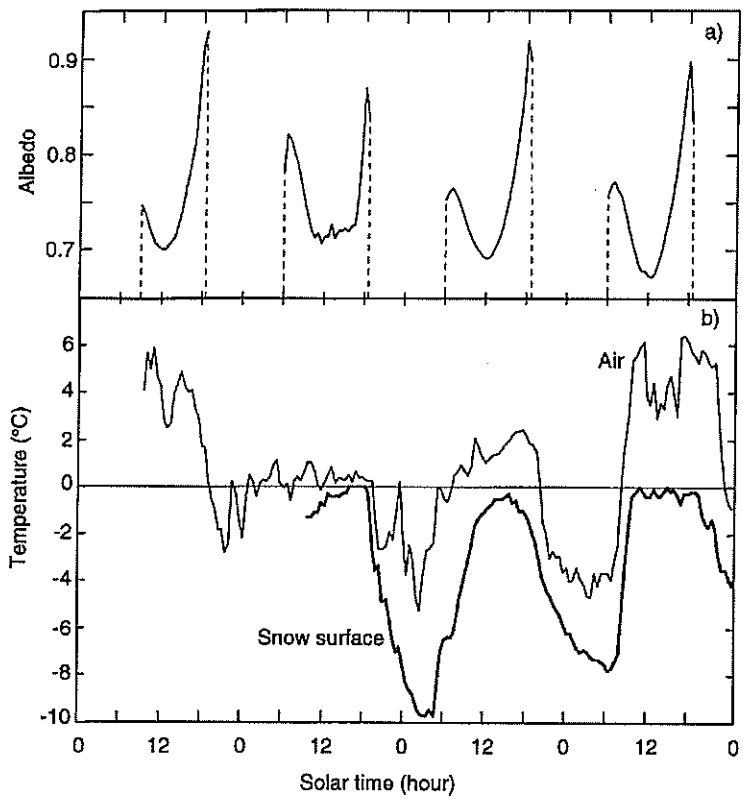

Figure 4 - Half-hourly averages of (a) albedo and (b) snow surface and air temperature measured at a height of 0.5 m on the névé of Franz Josef Glacier during 1 - 4 March 1992 [a) to d), respectively].

associated with snow surface temperatures of < - 2 °C; late afternoon surface temperatures were near 0°C. Minimum and maximum air temperatures of about - 5 and 6°C occurred about 2 h before sunrise and sunset, respectively (Fig. 4b).

Overnight air temperatures differed before the partly-cloudy day. There was an incursion of warm air at 0200 h, with air temperature rising above freezing to a maximum for the day of 1.2°C, 1.5 h before sunrise at 0630 h (snow surface temperature measurements did not begin until 1100 h). The minimum overnight air temperature of - 2.8°C was reached at 2300 h on 1 March. Early-morning albedos on 2 March varied between 0.79 and 0.82 and were generally similar in their relationship to solar zenith angle as albedos obtained during the afternoon of the cloud-free days (Fig. 5b). After 1000 h on this day, the sky was variable, but mostly cloudy, and albedo declined to a relatively constant value of about 0.72 .

Snow surface radiation balance

The largest term in the radiation balance was R_{si}, with a maximum of 965 W m^{-2} at 1200 h on a cloud-free day (Fig. 3a). However, the corresponding value of R_{so} was -675 W m^{-2}. Consequently, the maximum net shortwave radiation flux density was 290 W m^{-2}.

Modelled R_{li} varied by only 19% from an average value of 248 W m^{-2} (21 - 22 MJ m^{-2} d^{-1})(Fig. 6, Table 1). Variation in R_{li} was proportional to

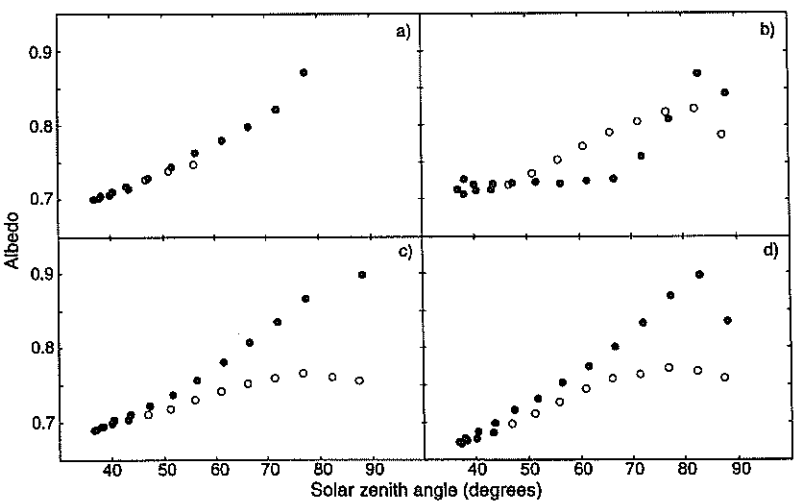

Figure 5 - The relationship between albedo and solar zenith angle on the névé of Franz Josef Glacier during 1 - 4 March 1992 [a) to d), respectively]. Open and closed symbols are for morning and afternoon data, respectively.

Table 2 - Some characteristics of surface snow that fell onto the névé of Franz Josef Glacier during 28 and 29 February 1992.

Depth (m)	Grain Shape (form)	Grain Diameter (mm)	Density (kg m^{-3})
1 March 1992 at 1330 h			
0.005	melted	1.0	500
0.05	melted	0.3	350
0.10	rounded	0.2	330
0.15	rounded	0.2	230
0.20	rounded	0.2	320
0.25	rounded	0.2	300
0.30	rounded	1.0-1.5	530
2 March 1992 at 1030 h			
0.005	rounded	0.7	460
0.05	rounded	0.3	390
0.10	rounded	0.2	410
0.15	rounded	0.2	420
0.20	rounded	0.1	230
0.25	rounded	0.1	190
0.30	rounded	0.8-1.0	550
3 March 1992 at 1000 h			
0.005	melted	1.0	490
0.05	rounded	1.2	490
0.10	rounded	0.3	430
0.15	rounded	0.2	430
0.20	rounded	0.1	500
0.25	rounded	0.8	460
0.30	rounded	1.2	620
4 March 1992 at 1030 h			
0.005	melted	1.3	410
0.05	melted	1.0	410
0.10	rounded	0.8	380
0.15	rounded	0.8	450
0.20	rounded	1.0	550
0.25	rounded	1.1	560
0.30	rounded	1.1	600
5 March 1992 at 1030 h			
0.005	melted	1.0	400
0.05	rounded	0.8	420
0.10	rounded	0.7	450
0.15	rounded	0.8	480
0.20	rounded	1.0	470
0.25	rounded	1.2	570
0.30	rounded	0.8	570

variation in air temperature, which largely determined the calculated value of atmospheric emissivity. Overall, modelled values were within 10% of that calculated as a residual of equation (1), with measurements of the other four terms. The average value of R_{lo} was -301 W m^{-2} (range = 43 W m^{-2}). Therefore, net longwave radiation was generally about -50 W m^{-2} (-4 to -5 MJ m^{-2} d^{-1}).

The range of R_n was -88 to 162 W m^{-2}. Maximum values were obtained at about 1100 h on the cloud-free days. Minimal R_n was generally constant between -60 and -80 W m^{-2} throughout cloud-free nights. However, during the early morning of 2 March, R_n increased to -25 W m^{-2} between 0200 and 0500 h, suggesting the presence of clouds (Fig. 6b). Although daytime total R_n was 1.8 - 2.6 MJ m^{-2} each day, there was a daily (24 h) net loss of all-wave radiation on 2 and 3 March (-0.6 and -0.3 MJ m^{-2} d^{-1}) and only a small net gain of radiant energy on 4 March (0.5 MJ m^{-2} d^{-1}).

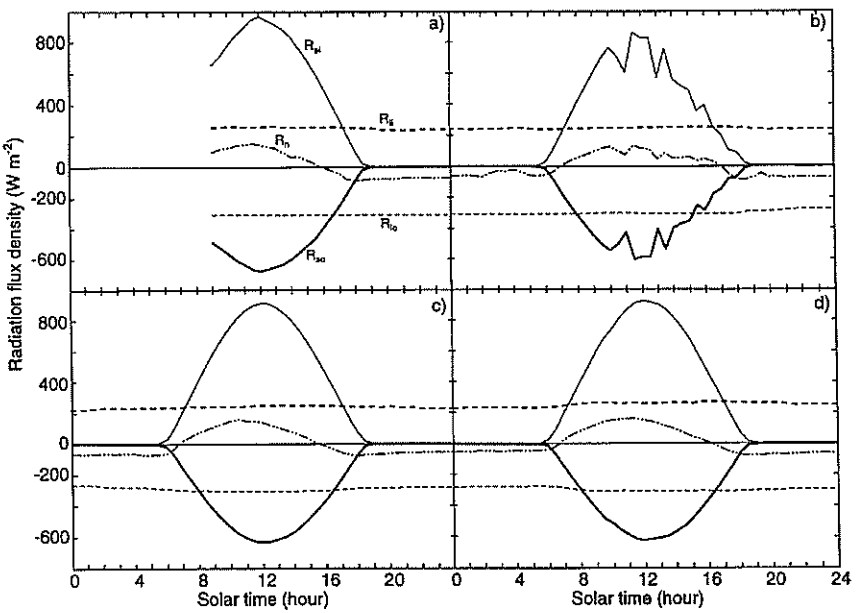

Figure 6 - Hourly averages of measured net all-wave (R_n), incoming shortwave (R_{si}), outgoing shortwave (R_{so}), and outgoing longwave (R_{lo}) radiation on the névé of Franz Josef Glacier during 1 - 4 March 1992 [a) to d), respectively]. Also shown for the four days is hourly incoming longwave radiation (R_{li}) estimated using the cold temperature model of Satterlund (1979).

Attenuation of visible radiation in snow

The measurements of radiation penetrating the snow pack were completely reliable only on 2 March because ablation and melt later exposed some of the diodes. Attempts to re-cover exposed diodes with snow gave uncharacteristic capricious radiation profiles. Normalised to the snow surface irradiance, radiation profiles were virtually identical at 0900 and 1200 h when the sky was cloud-free and solar zenith angles were 56 and 37°, respectively (Fig. 7). About 15 % of incident radiation penetrated to a depth of 0.07 m and 1 % to 0.3 m, the base of the new-fallen snow. Some cloud was present during the 1500 and 1800 h profiles (the ratios of measured R_{si} to clear-sky R_{si} were 0.65 and 0.52, respectively) and solar zenith angles were 52 and 83°. Consistently higher percentages of irradiance then reached depths of 0.11 and 0.15 m.

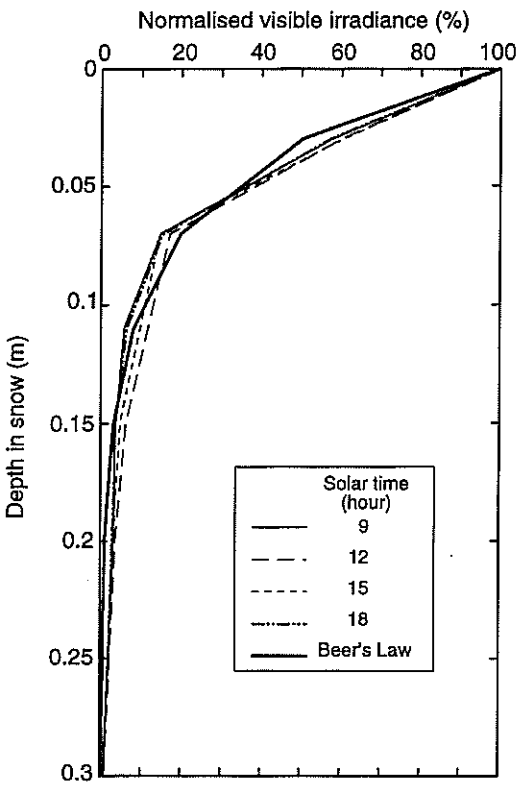

Figure 7 - The relationship between normalised visible irradiance (%) and depth (m) in 0.3 m of recently fallen snow on the névé of Franz Josef Glacier at 9, 12, 15 and 18 hours on 2 March 1992. Also shown are modelled estimates using Beer's Law with an attenuation coefficient of 23 m^{-1}.

The attenuation of radiation (R) in a homogeneous translucent medium is exponential according to Beer's Law, with $R(z) = R(0)\, e^{-kz}$ where R(0) is surface irradiance and z is depth. The data suggested that a visible radiation attenuation coefficient (k) was 23 m^{-1}. The exponential model consistently under-estimated irradiance at depth 0.03 m and over-estimated irradiance at depth 0.07 m by 44 and 24 W m^{-2}, on average. Modelled irradiance was within 10 W m^{-2} of the measurements for the four lower depths.

Ablation

Because of melting snow, the acoustic sensor stand was unstable during the first three days of measurements. A complete day of reliable 30-min ablation (surface lowering) data was obtained only on 4 March. On this day, ablation was largely confined to the daylight hours (Fig. 8). Between 0600 and 1700 h, the ablation rate was relatively constant at about 3 mm (depth) h^{-1}. Acoustic ablation measurement at the 30-min time step did include some noise and the apparent snow surface rose (negative ablation) on four occasions by 0.5 - 2 mm. Daily total ablation measured using the acoustic sensor was 32 mm, in agreement with the corresponding average of 30 mm (± 3 mm standard deviation) measured using the stakes. The

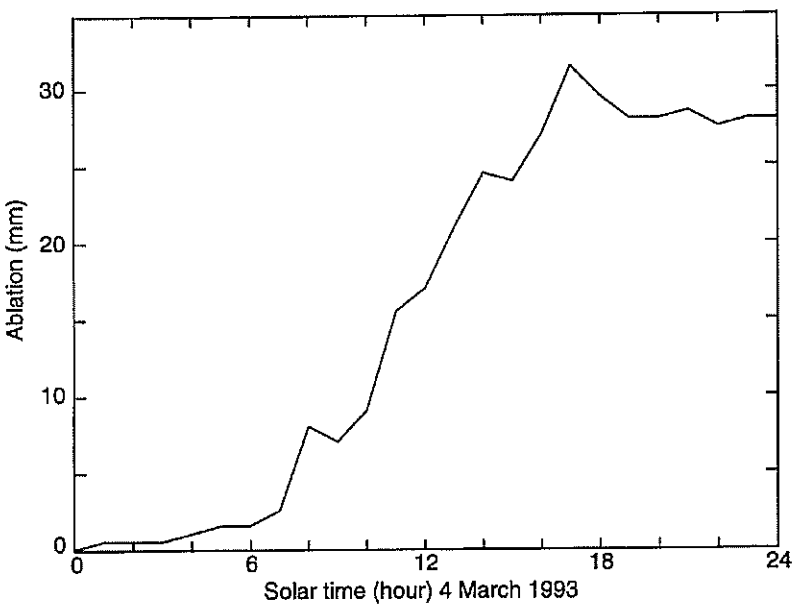

Figure 8 - The diurnal course of cumulative ablation (lowering of the snow surface, mm) on the névé of Franz Josef Glacier during 4 March 1992, measured with an acoustic sensor.

stake measurements also showed that nearly all ablation took place during the daytime. There was 69 mm (depth) of daytime ablation during 0700 - 1900 h, 2 - 4 March, or 23 mm d^{-1}. By contrast, there was only about 1 mm of ablation during each 12-h night. Variability amongst the 10 stakes was small, and the standard deviation of 3-day ablation rates was only 9% of the average. Snow density tended to increase over the study period, especially following the rainfall and near-surface cloud on 2 March when there may have been condensation onto the snow from the warm, moist air, and snow compaction. Some surface lowering may thus not be attributable to snowmelt (Table 2).

Discussion

Because nearly all the 23 mm d^{-1} ablation took place during the daytime, it appears that radiation, which in turn drives sensible, latent, and conductive heat fluxes, largely determines alpine snowfield ablation under fine summertime conditions. This is also apparent from the diurnal variations associated with wind speed, air specific humidity (Fig. 9) and air temperature (Fig. 4). The high rate of ablation suggests that melt is likely to have been the principal cause of ablation. An order of magnitude more energy would be required for sublimation (the latent heat of sublimation = 2.83 MJ kg^{-1} at 0°C) to produce the measured ablation rates. We can express the daytime net radiation in terms of an equivalent ablation rate by dividing by the latent heat of fusion (0.333 MJ kg^{-1} at 0°C) and the surface snow density (c. 450 kg m^{-3}, Table 2). This calculation ignores the contribution of melting at greater depths in the snow pack because little visible radiation penetrated below the near-surface layer (Fig. 7). Average daytime R_n = 2.1 MJ m^{-2} (Table 1) converts to an ablation rate equivalent of 14 mm d^{-1}. Consequently, we estimate that daytime R_n contributed 61% of the energy used for ablation.

Other studies indicate that R_n generally supplies 50 - 60% of the energy for surface melt of temperate-zone glaciers during summer. During fine summer days, R_n contributed 50 - 60% of the melt energy for a clean blue ice surface at the Franz Josef Glacier terminus (elevation 500 m), but considerable nighttime ablation occurred there as well, and sensible heat flux was the principal energy source on a 24-h basis (Isikawa *et al.*, 1992). Over 53 days during two summer periods, R_n supplied 52% of the melt energy at 1500 m elevation on the Ivory Glacier, which is located about 80 km north of the study site (Hay and Fitzharris, 1988a). The rest of the melt energy during fine weather was supplied by convection through sensible and latent heat fluxes (34 and 12%, respectively, with the remaining 2% being energy from rain; Hay and Fitzharris, 1988b). Synoptic-scale weather was also influential: radiation energy was most important for melt

at the Ivory Glacier site during southerly atmospheric circulation patterns with cool, dry air flow and mostly clear skies, while convective energy was more important during northerly circulations with warm, moist air flow with more cloudy conditions (Fitzharris *et al.*, 1992). At a fresh snowpack site at 2500 m elevation on the Peyto Glacier in Canada (51°40'N, 116°33'W), R_n accounted for 48% of the energy used in snow melt over 24 h during 8 summer days (Munro, 1990).

Albedo (R_{si}/R_{so}) was the most important determinant of the snow radiation balance. Our values of albedo are comparable to recently fallen snow data from temperate and sub-arctic latitudes (Table 3). Albedo increased with increasing solar zenith angle. This can be understood by examining the light scattering process in snow, as explained by Warren (1982). He reasoned that with low sun, a photon of light would be expected to undergo its first scattering event close to the snow surface because it entered the snow at a grazing angle. Scattering tends to be within a few degrees of the forward direction, thus enhancing the photon's chance of escaping the snow.

In our study, albedo was significantly greater during the late afternoon than during the early morning for a given solar zenith angle. Snow albedo:solar zenith angle hysteresis has been observed elsewhere, but the highest albedo values were measured during the early morning (e.g., Hubley, 1955; McGuffie and Henderson-Sellers, 1985). McGuffie and Henderson-Sellers hypothesised that in the early morning a frozen snow surface increased specular reflection. Hubley observed a thin, icy crust surface at his glacier site during clear nights, and we believe that the specular reflection argument is predicated on the early morning snow surface being relatively smooth, as would occur with the formation of rime or firnspiegel. Our asymmetry in the diurnal variation of albedo was associated with snow surface temperatures < - 2°C in the early morning, and late afternoon (wet) surface temperatures near 0°C. We postulate that spatially variable crystal growth of early morning hoarfrost after calm clear cold nights roughened the snow surface, and decreased specular reflection, trapping more shortwave radiation than the melting surface film of water that had developed by the afternoon. The formation of hoarfrost was probably caused by an influx of humid maritime air because the Tasman Sea is located only 25 km to the west of our site. Hoarfrost formation was also the result of low wind speeds (Fig. 9), low snow surface temperatures (Fig. 4; and corresponding low surface saturation specific humidities), and relatively high air specific humidity (Fig. 9) at our site in early morning. The effects of snow surface metamorphism on albedo should be investigated.

The attenuation of visible radiation in recently fallen snow generally

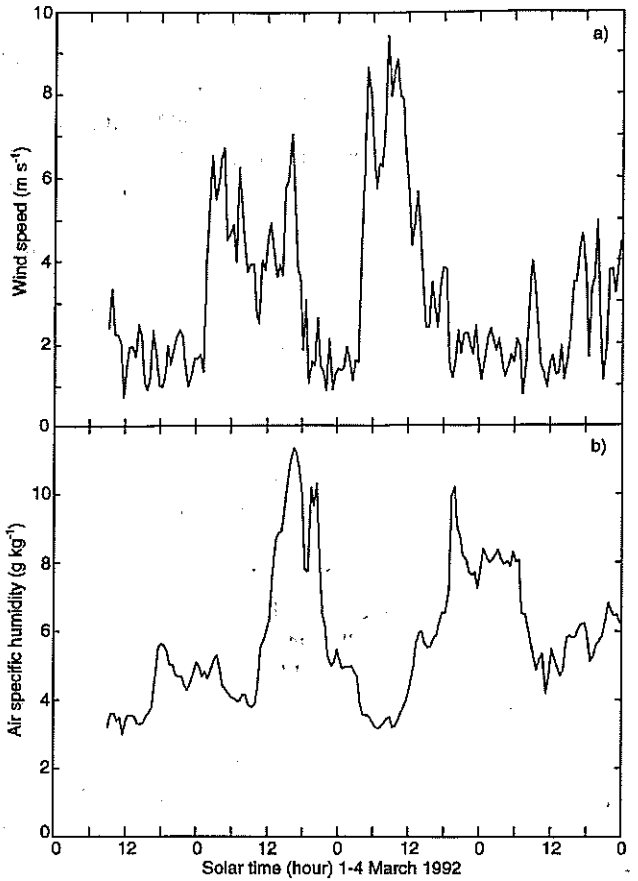

Figure 9 - Half-hourly averages of (a) wind speed at a height of 1.8 m and (b) air specific humidity at a height of 0.5 m on the névé of Franz Josef Glacier during 1 - 4 March 1992. Average atmospheric pressure was equal to 80 kPa.

Table 3 - Daily averages and daytime ranges of the albedo of recently fallen snow.

Site	Latitude, Longitude	Elevation (m)	Albedo Daily Average	Albedo Daytime Range	Source
Resolute, NWT Canada	74°43'N, 94°59'W	64	0.70	06.0-0.80	Dubreuil & Woo 1984
Central Sierra, CA USA	39°22'N, 120°22'W	2100	0.55-0.84	-	Aguado 1985
Terre Adelie, Antarctica	67°23'S. 138°43'E	1560	0.90	0.81-0.92	Wendler & Kelly 198
St. Paul, MN USA	44°59'N, 93°11'W	296	0.80	-	Baker *et al.* 1990
South Pole, Antarctica	90°00'S	2800	0.90	0.83-0.97	Carroll & Fitch 1981
Franz Josef Glacier Névé New Zealand	43°24'S, 170°12'E	2150	0.75	0.67-0.93	This study

followed Beer's Law, but agreement between measured and modelled irradiance was best below a depth of about 0.1 m, in accordance with other snow studies (e.g. Brandt and Warren, 1993). The attenuation coefficient (k) was equal to 23 m^{-1} and was related to snow grain size. According to Schwerdtfeger and Weller (1977), light scattering is the primary process determining radiation attenuation in snow. They argue that scattering rate is inversely proportional to grain size, leading to an inverse relationship between k and grain diameter (s). The dimensionless product (ks) varied between 0.020 and 0.030 at Plateau Station, Antarctica (Schwerdtfeger and Weller 1977). Our data support their argument: using our value of $k = 23\ m^{-1}$ and taking surface snow s = 1 mm from Table 2, we find that (ks) = 0.023 for the Franz Josef névé.

The diffuse shortwave radiation component was higher than expected for an alpine site in a remote, maritime, and pollution-free environment. For a clean, cloudless sky and solar zenith angle < 50°, the ratio of diffuse to total shortwave radiation is 0.10 to 0.15, according to Monteith and Unsworth (1990). Our 1000 - 1400 h clear-sky measurements for solar zenith angles of 37 - 47° indicated a relatively constant diffuse ratio of 0.19. One possible explanation was a higher stratospheric aerosol concentration during field measurements because of the June 1991 Mt. Pinatubo (Philippines) and the August 1991 Mt. Hudson (Argentina) volcanic eruptions (Minnis *et al.*, 1993). At Lauder, New Zealand, located about 180 km south of our site (45°S, 173°E), the 400 - 450 nm waveband diffuse to total irradiance ratio increased by up to a factor of two during July 1991 - June 1992 compared with data from the previous year (McKenzie, 1992). A second explanation involves multiple reflection, possibly enhanced by reflection from adjacent above-horizon snow-covered surfaces (see Figs. 1 and 2), whereby reflected shortwave radiation is scattered by air molecules back onto the surface. This Rayleigh scattering process can be significant over high albedo surfaces like snow (McCullough and Porter, 1971; Kierkus and Colborne, 1989).

This study drew upon detailed measurements made at a single, well-instrumented site. However, direct measurement of net radiation is not always possible. Our use of measurements and modelling to determine radiation balance components showed how it may be estimated accurately. Shortwave irradiance can readily be calculated (Fig. 2), and albedo is related to snow morphology and solar zenith angle. Using Satterlund (1979) and the Stefan-Boltzmann Law, net longwave radiation for snow surfaces can be approximated from simple climate variables (Table 1). For snow energy balance and ablation models used for the polar regions and in global climate models, data may be available only from satellite sensors. The relationships developed in this paper contribute useful information for calculating energy exchange rates between the atmosphere and snow and glacier surfaces.

Conclusions

Albedo was the most important determinant of the snow surface radiation balance on the névé of Franz Josef Glacier. The formation of hoarfrost on cold mornings and snow surface melting during the afternoon affected the relationship between albedo and solar zenith angle; albedo was significantly greater during the late afternoon than during the early morning. To a first approximation, the attenuation of visible radiation in recently fallen snow followed Beer's Law with an attenuation coefficient that was equal to 23 m^{-1} and was related to snow grain size. Virtually no visible radiation penetrated through 0.3 m of recently fallen snow to the underlying older snow and ice. Nearly all of the 23 mm d^{-1} ablation occurred between sunrise and sunset. Daytime net radiation was estimated to supply about 60% of the energy for surface melt under fine summertime conditions on the alpine snow field.

Acknowledgements

We thank the New Zealand Foundation for Research, Science, and Technology for providing funds to Manaaki Whenua - Landcare Research, and the University of Canterbury for its support of the Geography Department. We are very grateful to Mr T. Trewinnard of Blue Skies Weather & Climate Services Ltd., Christchurch for his excellent weather forcasts that helped us to safely conduct measurements at a remote, alpine site that was a six-hour drive and over the main divide from our laboratories. Dr. Blair Fitzharris, James Barringer, Joanna Orwin, Eileen McSaveney and two reviewers provided many helpful comments on the manuscript. Final mousework on the figures was done by Tom Pearson.

References

Aguado, E. 1985: Radiation balances of melting snow covers at an open site in the Central Sierra Nevada, California. *Water Resources Research 21*: 1649-1654.

Baker, D.G.; Ruschy, D.L.; Wall, D.B. 1990: The albedo decay of prairie snows. *Journal of Applied Meteorology 29*: 179-187.

Brandt, R.E.; Warren, S.G. 1993: Solar-heating rates and temperature profiles in Antarctic snow and ice. *Journal of Glaciology 39*: 99-110.

Carroll, J.J.; Fitch, B.W. 1981: Dependence of snow albedos on solar elevation and cloudiness at the South Pole. *Journal of Geophysical Research 86*: 5271-5276.

Chinn, T.J.H. 1995: Glacier fluctuations in the Southerns Alps of New Zealand determined from snowline elevations. *Arctic and Alpine Research 27*: 187-198.

Colbeck, S.C.; Akitaya, E.; Armstrong, R.; Gubler, H; Lafeuille; Lied, K; McClung, D.; Morris, E. 1990: The international classification for seasonal snow on the ground. International Commission on Snow on Ice of the International Association of Hydrological Sciences, Wallingford, UK, 23 p.

Drummond, A.J. 1956: On the measurement of sky radiation. *Archiv fur Meteorologie,Geophysik und Bioklimatologie, Series B 7*: 413-436.

Dubreil, M.-A.; Woo, M. 1984: Problems of determining snow albedo for the high Arctic. *Atmosphere-Ocean 22*: 379-386.

Fitzharris, B.B. 1987: A method for indexing the variability of alpine snow cover over large areas. In: Large Scale effects of Seasonal Snowcover, International Association of Hydrological Sciences Publication 166: 139-150.

Fitzharris, B.B.; Hay, J.E.; Jones, P.D. 1992: Behaviour of New Zealand glaciers and atmospheric circulation changes over the past 130 years. *The Holocene 2*: 97-106.

Fitzharris, B.B.; Owens, I.F.; Chinn, T.J.H. 1992: Snow and glacier hydrology. In: Mosley, M.P. (ed.), Waters of New Zealand, New Zealand Hydrological Society: Wellington, 75-93.

Gates, D.M. 1980: *Biophysical Ecology*. New York: Springer-Verlag. 611 pp.

Griffiths, G.A.; McSaveney, M.J. 1983: Distribution of mean annual precipitation across some steepland regions of New Zealand. *New Zealand Journal of Science 26*: 197-209.

Hay, J.E.; Fitzharris, B.B. 1988a: The synoptic climatology of ablation on a New Zealand glacier. *Journal of Climatology 8*: 201-215.

Hay, J.E.; Fitzharris, B.B. 1988b: A comparison of the energy-balance and bulk-aerodynamic approaches for estimating glacier melt. *Journal of Glaciology 34*: 145-153.

Horowitz, J.L. 1969: An easily constructed shadow-band for separating direct and diffuse solar radiation. *Solar Energy 12*: 543-545.

Hubley, R.C. 1955: Measurements of diurnal variations in snow albedo on Lemon Creek Glacier, Alaska. *Journal of Glaciology 2*: 560-563.

Ishikawa, N.; Owens, I.F.; Sturman, A.P. 1992: Heat balance characteristics during fine periods on the lower parts of the Franz Josef Glacier, South Westland, New Zealand. *International Journal of Climatology 12*: 397-410.

Kierkus, W.T.; Colborne, W.G. 1989: Diffuse solar radiation - Daily and monthly values as affected by snow cover. *Solar Energy 42*: 143-147.

McCullough, E.C.; Porter, W.P. 1971: Computing clear day solar radiation spectra for the terrestrial ecological environment. *Ecology 52*: 1008-1015.

McGuffie, K.; Henderson-Sellers, A. 1985: The diurnal hysteresis of snow albedo. *Journal of Glaciology 31*: 188-189.

McKenzie, R.L. 1992: UV spectral irradiance measurements in New Zealand: Effects of Pinatubo volcanic aerosol. In: Hudson, R.D. (ed), Proceedings 1992 Quadrennenial Ozone Symposium, 4 - 13 June 1992, Charlottesville, Virginia USA:627 - 630.

Male, D.H.; Granger, R.J. 1981: Snow surface energy balance. *Water Resources Research 17*: 609-627.

Minnis, P.; Harrison, E.F.; Stowe, L.L.; Gibson, G.G.; Denn, F.M.; Doelling, D.R.; Smith, Jr., W.L. 1993: Radiative climate forcing by the Mount Pinatubo eruption. *Science 259*: 1411-1419.

Monteith, J.L.; Unsworth, M.H. 1990. *Environmental physics*. 2nd ed. London: Edward Arnold. 291 pp.

Munro, D.S. 1990: Comparison of melt energy computations and alblatometer measurements on melting ice and snow. *Arctic and Alpine Research 22*: 153-162.

Reifsnyder, W.E. 1967: Radiation geometry in the measurement and interpretation of radiation balance. *Agricultural Meteorology 4*: 255-265.

Satterlund, D.R. 1979: An improved equation for estimating long-wave radiation from the atmosphere. *Water Resources Research 15*: 1649-1650.

Schwerdtfeger, P.; Weller, G.E. 1977: Radiative heat transfer processes in snow and ice. In Businger, J.A. (ed.), Meteorological studies at Plateau Station, Antarctica, *American Geophysical Union, Antarctic Research Series 25*: 35-39.

Stanhill, G. 1985: Observations of shade-ring corrections for diffuse sky radiation measurements at the Dead Sea. *Quarterly Journal of the Royal Meteorological Society 111*: 1125-1130.

Steven, M.D. 1984: The anisotropy of diffuse solar radiation determined from shade-ring measurements. *Quarterly Journal of the Royal Meteorological Society 110*: 261-270.

Warren, S.G. 1982: Optical properties of snow. *Reviews of Geophysics and Space Physics 20*: 67-89.

Wendler, G.; Kelley, J. 1988: On the albedo of snow in Antarctica: A contribution to I.A.G.O. *Journal of Glaciology 34*: 19-25.

Manuscript received: 29 August 1995; accepted for publication: 9 January 1996.